

# RSC Advances



This is an *Accepted Manuscript*, which has been through the Royal Society of Chemistry peer review process and has been accepted for publication.

*Accepted Manuscripts* are published online shortly after acceptance, before technical editing, formatting and proof reading. Using this free service, authors can make their results available to the community, in citable form, before we publish the edited article. This *Accepted Manuscript* will be replaced by the edited, formatted and paginated article as soon as this is available.

You can find more information about *Accepted Manuscripts* in the [Information for Authors](#).

Please note that technical editing may introduce minor changes to the text and/or graphics, which may alter content. The journal's standard [Terms & Conditions](#) and the [Ethical guidelines](#) still apply. In no event shall the Royal Society of Chemistry be held responsible for any errors or omissions in this *Accepted Manuscript* or any consequences arising from the use of any information it contains.

# Investigation of the growth temperature on indium diffusion in InGaAs/GaAsP multiple quantum wells and photoelectric properties

Hailiang Dong,<sup>a,b</sup> Jing Sun,<sup>a,b</sup> Shufang Ma,<sup>a,b</sup> Jian Liang,<sup>a,b</sup> and Bingshe Xu<sup>a,b\*</sup>

<sup>a</sup> Key Laboratory of Interface Science and Engineering in Advanced Materials, Taiyuan University of Technology, Ministry of Education, Taiyuan, Shanxi 030024, P. R. China

<sup>b</sup> College of Materials Science and Engineering, Taiyuan University of Technology, Taiyuan, Shanxi 030024, P. R. China

InGaAs/GaAsP multiple quantum wells (MQWs) structures were grown by metal-organic chemical vapor deposition and the effect of the growth temperature on the interfacial crystal quality was characterized by high-resolution X-ray diffraction and photoluminescence. Surface roughness of MQWs was measured by atomic force microscopy for evaluating the surface quality. The existence of indium diffusion zone (InGaAsP) between InGaAs and GaAsP was demonstrated by secondary ion mass spectrometry profiles in growth direction. The results suggest the different diffusion width originate from the growth temperature variation. The smoother surface and higher quality interface of MQWs was obtained at 650 °C growth temperature. Furthermore, the phenomenons of current self-oscillations were confirmed through current-voltage (I-V) measurement at room temperature, which can be attributed to the negative differential resistance effect. The influence of the growth temperature on the crystal quality of InGaAs/GaAsP MQWs were used for the optimization of technological parameters.

**Key words:** Multiple quantum wells; Strain mismatch; Interface

## Introduction

InGaAs/GaAsP MQWs heterojunction is crucial in the fabrication of many optoelectronic devices, such as laser,<sup>1-3</sup> solar cells modulators<sup>4-7</sup> and photodetectors.<sup>8-9</sup> The key of this study is to address the difficulty in the formation of abrupt InGaAs/GaAsP heterointerfaces, particularly when utilizing high phosphorus and indium content.<sup>10</sup> The unintentional InGaAsP interfacial layers that interlope on InGaAs wells and GaAsP barriers could be introduced by switching column V flow or indium (In) atomic diffusion at interface. Many experiments were devoted to improving high quality abrupt interfaces of InGaAs/GaAsP. Joshua et al proposed a thick GaAs interfacial transition layer, which can

---

\* Corresponding author: Key Laboratory of Interface Science and Engineering in Advanced Materials, Taiyuan University of Technology, Taiyuan, Shanxi 030024, PR China. Tel: +86-351-601 0311; Fax: +86-351-601 0311.  
E-mail address: [xubs@tyut.edu.cn](mailto:xubs@tyut.edu.cn) (B. S. Xu)

prevent phosphorus carry-over and indium diffusion between the barrier and well structures.<sup>11</sup> Fujii et al proposed a growth method to insert a gradual interlayers between InGaAs and GaAs with controlled atomic-layer thicknesses to avoid lattice relaxation for obtaining an abrupt interface of InGaAs/GaAsP.<sup>2</sup> Crystal defects were introduced by lattice mismatch and cumulative strain mismatch in InGaAs/GaAsP MQWs, which have a strong influence on In diffusion at interfaces.<sup>12</sup>

The optimization of growth conditions is still an issue, although many epitaxial processes were investigated on InGaAs/GaAsP MQWs quality dependence on alloy ordering and interface abruptness.<sup>3</sup> The complications partly arise from the thermodynamic and kinetic conditions in the reactor chamber, which strongly affect the composition uniformity and the interface sharpness.<sup>7-8</sup> Thus, the difficulty comes from the fact that a number of different phenomena, both physical and technological, require modulating during the epitaxial process. The epitaxial process influence on segregation and desorption efficiency of InGaAs well is different. Therefore, an effective solution is put forward from optimization of the growth temperature, as well as the growth rate,<sup>13-14</sup> growth interruption<sup>15,16</sup> and V/III ratio.<sup>13</sup> The correlation between the In segregation and growth temperature was informed by previous reports,<sup>17-19</sup> which indicate In diffusion is mainly affected by the growth temperature. Thus, InGaAs/GaAsP MQWs with an abrupt interface is obtained through the optimization of growth temperature, which was reported by Ebert et al in Refs. [20]. When InGaAs/GaAsP MQWs were grown at high growth temperature, the crystal and optical quality of epilayers is improved. But InGaAsP interfacial layers were easily obtained and the probability of rough hetero-interfaces and of more defects increase.<sup>21</sup> Meanwhile, In diffusion and segregation at interface become more serious. However, in order to suppress In diffusion at interface, a large amount of unintentional impurities (such as oxygen,<sup>22</sup> methyl radicals<sup>15</sup>) were incorporated into crystal lattice at low growth temperature, which affects crystal quality and optical performance of MQWs. Furthermore, the incorporation of impurities at low temperature can result in the formation of island mode, but not desirable, because of the higher interface roughness.<sup>23-24</sup> In order to avoid plastic relaxation of strained MQWs, the growth mode has to be performed in step-flow regime. While the effect of interdiffusion on the interface and the segregation and desorption of In atoms are suppressed at low growth temperatures. Therefore, the growth temperature plays a role in growth of InGaAs/GaAsP MQWs for obtaining an abrupt interface. The effect of diffusion and segregation of indium is suppressed through the optimization of growth temperature so that the high crystal quality of InGaAs/GaAsP MQWs is grown.<sup>20</sup>

In this paper, we studied the optimization of growth temperature to produce high quality and abrupt heterointerface of InGaAs/GaAsP MQWs. Three samples grown at different growth temperature were compared in order to estimate the influence on the width of In diffused interface and surface roughness. The formation mechanism of In diffused interface was also discussed.

## Experiment

InGaAs/GaAsP MQWs were epitaxially grown on (100) n-type GaAs substrates misoriented 15° towards [110] by MOCVD using trimethylgallium (TMGa), trimethylindium (TMIn), arsine (AsH<sub>3</sub>), phosphine (PH<sub>3</sub>) and high-purity H<sub>2</sub> carrier gas at different growth temperature of 620 °C , 650 °C and 680 °C, separately. The structure of the InGaAs/GaAsP MQWs is illustrated in Fig. 1. The designed thicknesses and composition of InGaAs wells (10 nm and 0.14 in solid) and GaAsP barriers (10 nm and 0.20 in solid) remain constant for three samples.

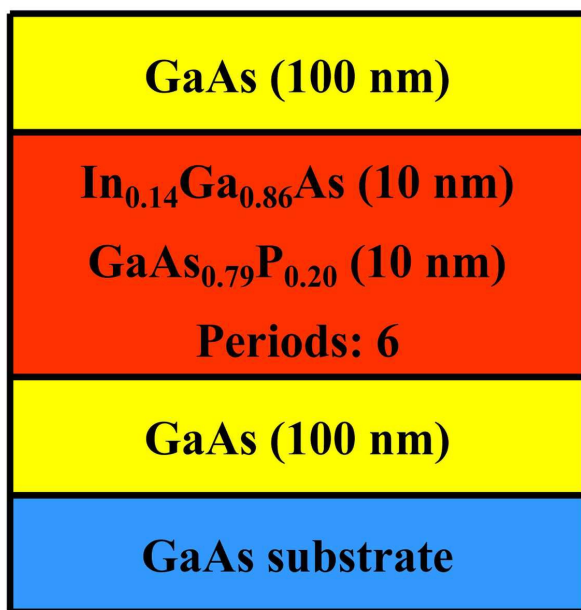
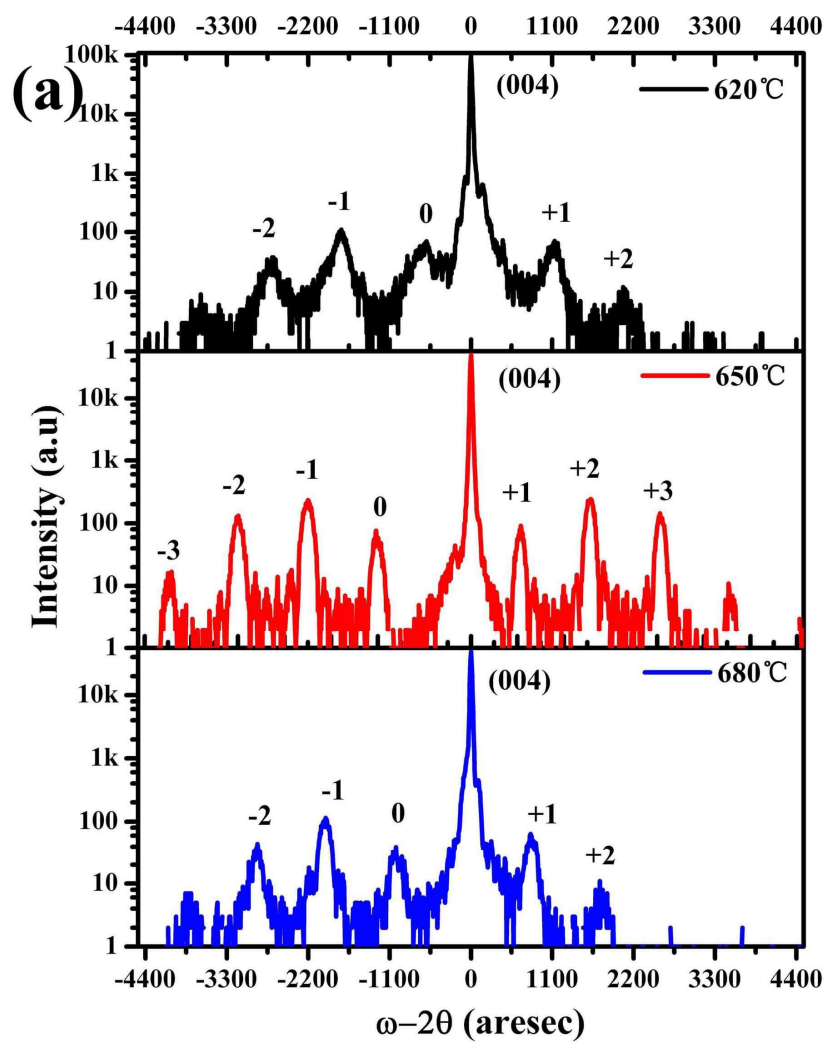


**Fig. 1** Schematic of InGaAs/GaAsP MQWs structure.

Three samples were analyzed by high-resolution X-ray diffraction (HRXRD) omega-2theta scanning of (004) planes in order to verify interfacial crystal quality, interface roughness, thickness, composition, and strain mismatch for each well and barrier of InGaAs/GaAsP MQWs. Surface reflectance curves were measured with a commercial system (EpiR-MTT, Laytec) for monitoring the transient behavior of surface morphology. The root mean square (RMS) surface roughness was characterized by atomic force microscope (AFM). Secondary ion mass spectrometry (SIMS) was used to analyze the diffused interfacial width in MQWs. The optical properties of MQWs were tested by photoluminescence (PL) spectroscopy with continuous-wave laser at 532 nm. The samples were

fabricated into  $5 \times 5 \text{ nm}^2$  mesas, and the current-voltage (I-V) characteristic were measured under current from 1 to 14 A at room temperature, using a AvaSpec-2048 fiber optic spectrometer.

## Results and discussion



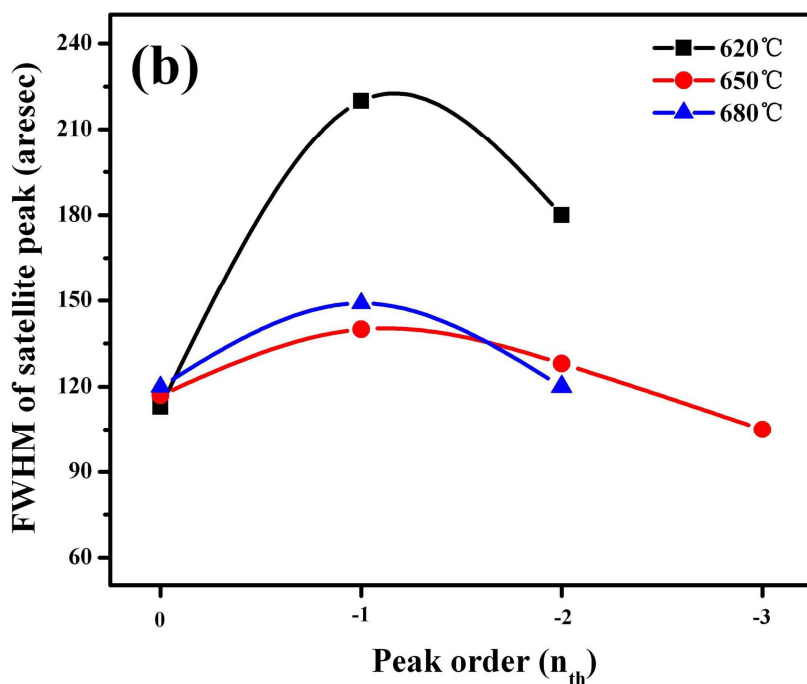


**Fig. 2**  $\omega/2\theta$  scans measured around the (004) symmetric HRXRD patterns (a) and dependence of the FWHM of satellite peaks on the satellite orders (b) of InGaAs/GaAsP MQWs grown at different temperatures. The symbols represent the experimental data and the solid lines are fit curves.

**Table 1.** The values of thickness, composition, strain mismatch and periodicity of samples obtained at 620 °C, 650 °C and 680 °C.

Samples	620 °C	650 °C	680 °C
InGaAs (nm)	10.01	10.00	9.93
GaAsP (nm)	10.06	10.02	10.08
Periodic thickness (nm)	20.07	20.02	20.01
InGaAs strain mismatch (ppm)	In <sub>0.138</sub> Ga <sub>0.862</sub> As (9894)	In <sub>0.135</sub> Ga <sub>0.865</sub> As (9679)	In <sub>0.133</sub> Ga <sub>0.867</sub> As (9535)
GaAsP strain mismatch (ppm)	GaAs <sub>0.898</sub> P <sub>0.202</sub> (-7259)	GaAs <sub>0.800</sub> P <sub>0.200</sub> (-7187)	GaAs <sub>0.801</sub> P <sub>0.199</sub> (-7151)
$\bar{\epsilon}$ average strain mismatch/period (ppm)	1296.1	1237.6	1129.5
$\epsilon_{\text{total}}$ accumulated strain mismatch (ppm nm)	$0.8305 \times 10^6$	$0.7664 \times 10^6$	$0.6352 \times 10^6$

To get an indication of the heterointerface quality for MQWs, the HRXRD FWHM plot as a function of peak order is also shown in Fig. 2 along with the HRXRD patterns. This approach for assessing the interface quality for GaN<sub>x</sub>As<sub>1-x</sub>/GaAs superlattices was reported in Refs. [25-26]. From the (004) symmetric HRXRD patterns of the samples in Fig. 2(a), the periodic thickness, compositions and strain mismatch are obtained by the simulation of the diffraction patterns, as listed in Table 1. In real MQWs, the interface roughness would broaden satellite peaks,<sup>27</sup> except for the zeroth-order one. If the interface roughness is described by a Gaussian distribution function with standard deviation  $\sigma$ , the FWHM of the  $n$ th peak will be expressed as<sup>28</sup>

$$W_n = W_0 + (\ln 2)^{1/2} n \Delta\theta_M \frac{\sigma}{\Lambda} \quad (1)$$

where  $n$  is the order of the satellite peak,  $\Lambda$  is the periodicity,  $\Delta\theta_M$  is the angle distance between adjacent satellite peaks, and  $\sigma/\Lambda$  is the interface roughness,  $W_0$  and  $W_n$  are the FWHM of zeroth- and  $n$ th-order peaks, respectively. The dependence of the FWHM of satellite peaks on the satellite orders from Fig. 2(a) shows a nonlinear relationship, as shown in Fig. 2(b). Because the difference of phase angle of atoms surface of two layers in face-centered cubic structure is  $180^\circ$ , which results in extinction phenomenon, the intensity of zero order satellite peak is weak.<sup>29</sup> It can be seen from the curve for 680 °C sample in Fig. 2(b) is very close to parabolic. According to formula (1), the interface roughness can be calculated from the FWHM of satellite peaks. Samples obtained at 620 °C and 680 °C have a relatively low interface roughness of 5.22 % and 2.78 %, respectively, while sample obtained at 650 °C has a much smaller value of 1.53 %. Therefore, the interfacial quality of the sample obtained at 650 °C is best among the three samples, and the corresponding interface roughness is minimum.



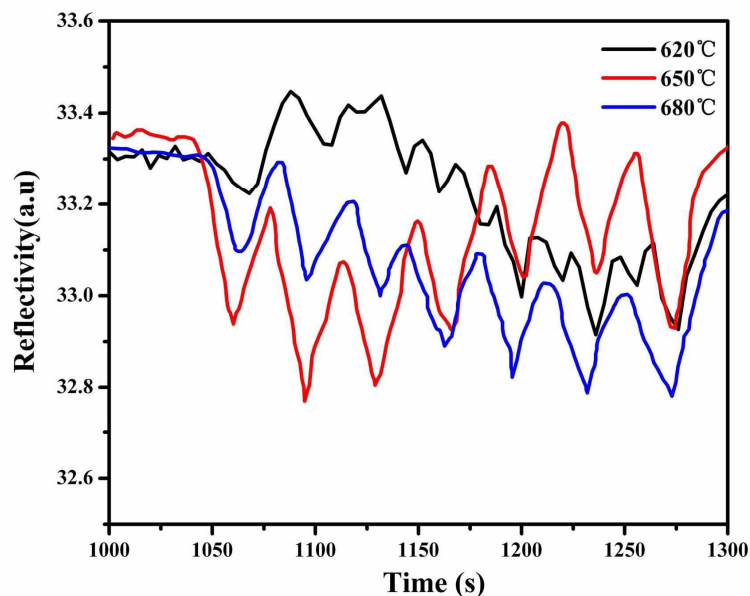
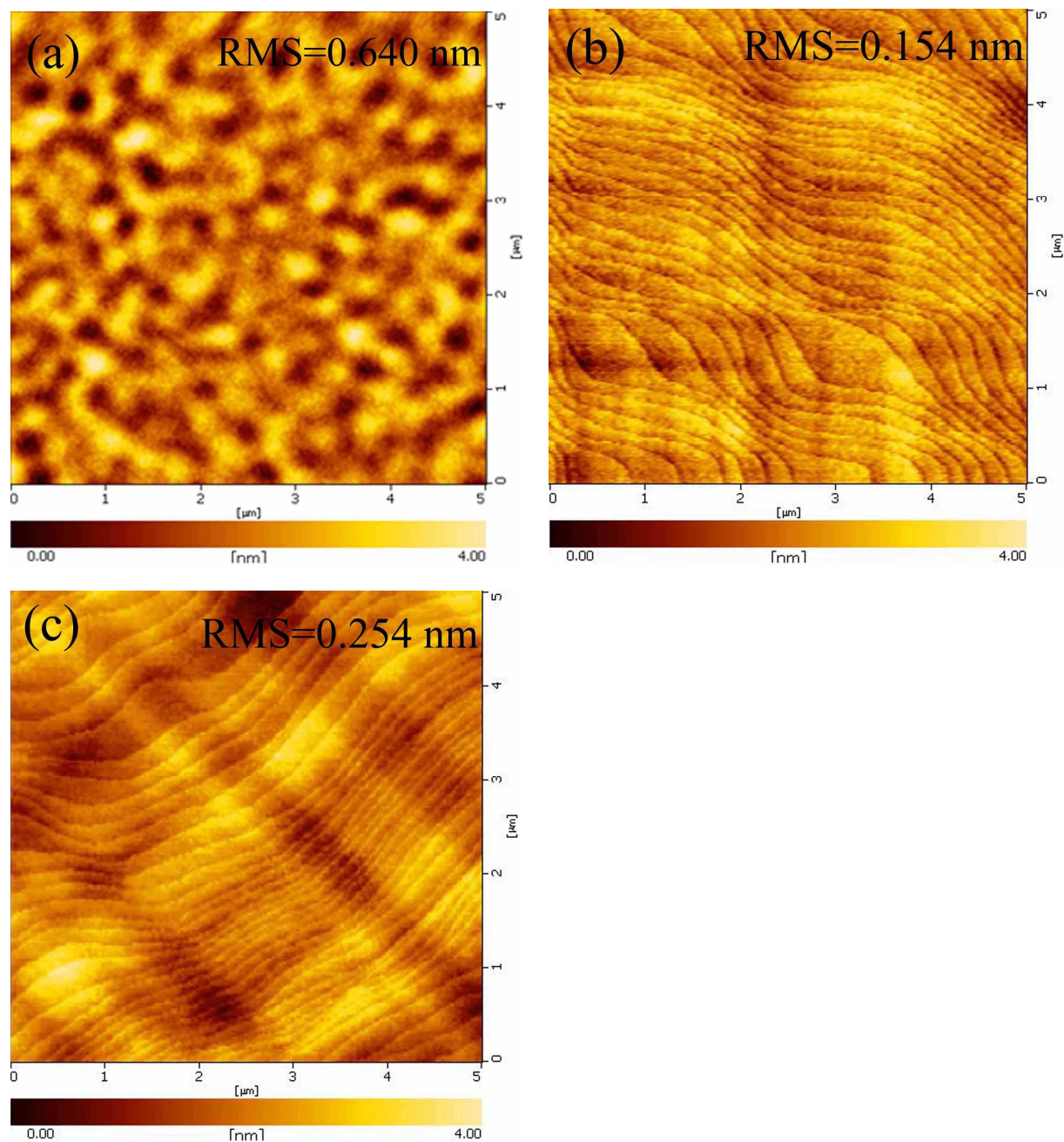


**Fig. 3** Time transient surface reflectivity during the growth of InGaAs/GaAsP MQWs structures at different growth temperatures.

In order to investigate the transient behavior of the surface in the course of growth, an in-situ optical surface reflectance facility was used to monitor surface morphology variation. For the three samples, surface reflectivities were measured in the course of growth, as shown in Fig. 3. All the reflectance values were normalized by the value on the GaAs surface at the initial of the MQWs' growth. A periodic feature is found for all the reflectance transients, which is the Fabry-Perot oscillation due to numerous reflections at hetero-interfaces.<sup>30</sup> The drop in surface reflectivity at a smaller number stacked quantum wells indicate incomplete strain balancing during the growth, as shown in Fig. 3 for 620 °C sample. This tendency was also observed for InGaAs/GaAsP quantum wells when the average strain exceeded +3000 ppm.<sup>31</sup> Once dislocations are introduced as the result of accumulated strain in MQWs, the surface morphology starts to degrade, resulting in decrease in surface reflectance. On the other hand, successful strain balancing results in no degradation in surface reflectance, as shown in Fig. 3 for 650 °C sample during the growth periods. When the surface reflectance value exhibits a subtle change the growth is terminated without any degradation in surface morphology, giving optimum strain-balanced MQWs. More impurities may be incorporated into MQWs during the course of reaction because of the lower growth temperature (620 °C), and defects increase so that the reflectivity values seriously drops and the periodic variation of reflectance curve deteriorates.<sup>32</sup> When MQWs are grown at higher growth temperature, thermal stress increase as the result of lattice thermal mismatch



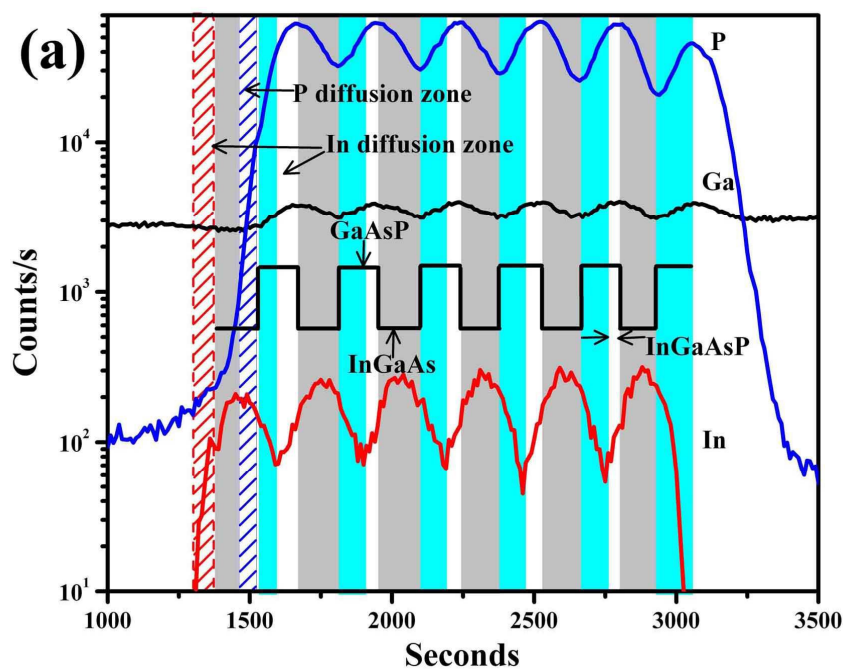
so that the reflectivity curve degrades, as shown in Fig. 3 for 680 °C sample, while the periodic reflectivity curve is a regular pattern. The relationship between transient surface reflectance and surface morphology in MQWs will be discussed in following AFM surface analysis.



**Fig. 4** The AFM images of InGaAs/GaAsP MQWs in  $5 \times 5 \mu\text{m}^2$  scan area with different growth temperature: (a)  $620^\circ\text{C}$ , (d)  $650^\circ\text{C}$  and (c)  $680^\circ\text{C}$ .

To verify growth model and evaluate surface roughness of MQWs, the surfaces of three samples at different growth temperature were analyzed by AFM and RMS roughness values are listed in Fig. 4. A notable feature is that RMS value is significantly improved at  $650^\circ\text{C}$  growth conditions (Fig. 3(b)). Furthermore, three-dimension (3D) growth model and two-dimension (2D) step-flow growth model

corresponding to sample 620 °C, 650 °C and 680 °C are observed from Fig. 4(a) and Fig. 4(b, c) respectively. In this way, 3D growth is suppressed as the growth temperature increases. However, a smooth surface could not be obtained because of the effects of impurities (e.g. oxygen in reaction chamber, arsine, phosphine or group III source) at 620 °C. The RMS roughness is improved by increasing growth temperature (650 °C), and twisted steps are observed with RMS=0.154 nm, as shown in Fig. 4(b). Then, the RMS roughness is not improved by further increasing growth temperature (680 °C), as shown in Fig. 4(c). A number of wide dark parallel belt structures on surface can be observed with the value of RMS=0.254 nm. The formation of dark groove belt can be explained by the distortion degree releasing the compressive stress in MQWs along with the increase of growth temperature. Combined with the reflectance measurement, the RMS value of MQWs for 620 °C sample is the largest agree with the reflectivity value drastically decrease. When the temperature increases to 650 °C, the strain-balanced MQWs are grown with low RMS value, and the reflectance curve is presented by regular periodic growth. While the growth temperature increases to 680 °C, the surface roughness increases, and the reflectance curve shows gradual decline. It indicates that there is slight In segregation or diffusion on InGaAs surface in growth direction. In atoms diffuse to the interface and are desorbed on the surface, which results in the interface roughening and broadening during the growth.



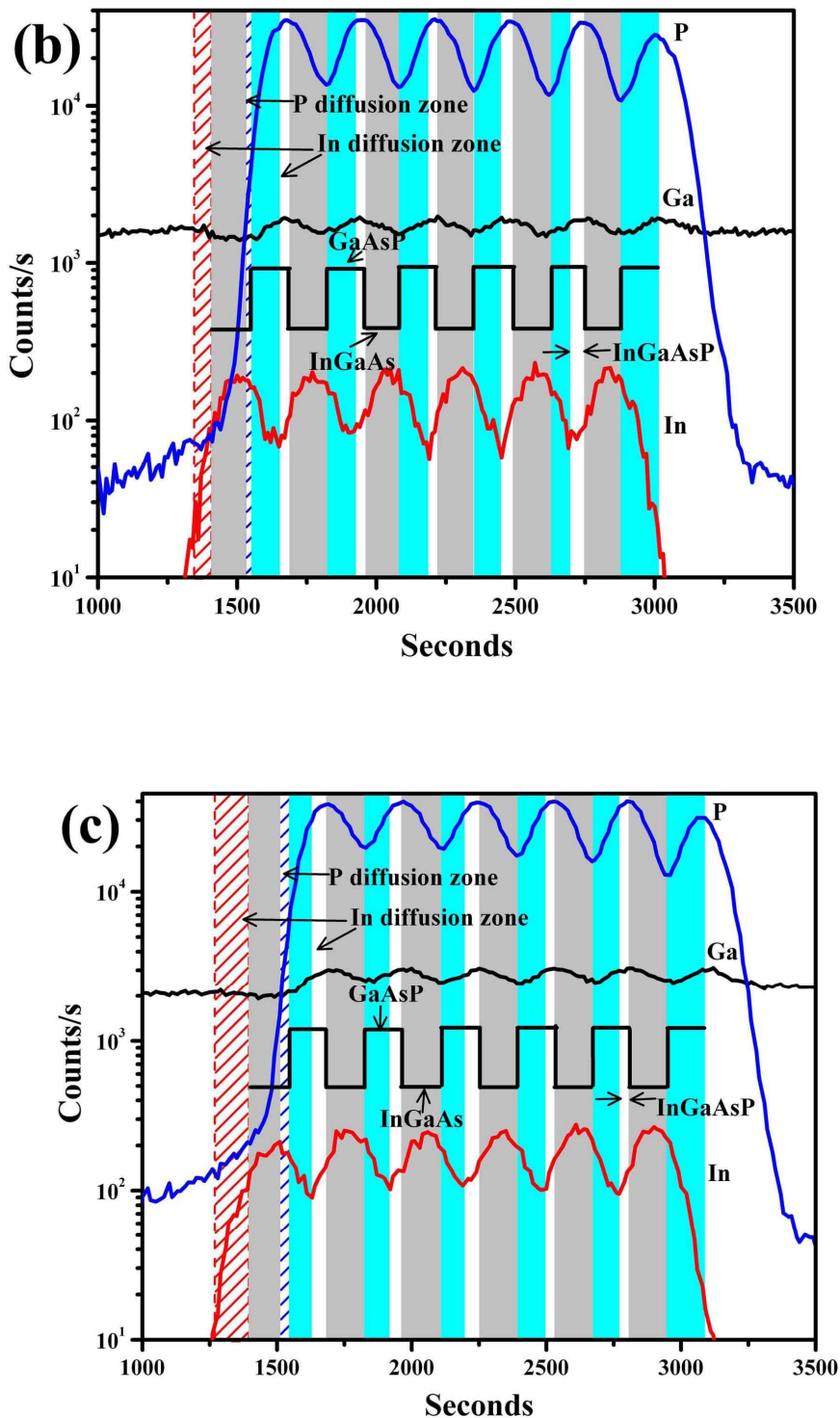


**Fig. 5** SIMS profiles of InGaAs/GaAsP MQWs with growth temperature 620 °C (a), 650 °C (b) and 680 °C (c) show the variation of phosphorous (P) (blue line), gallium (Ga) (black line), and indium (In) (red line). Indium diffusion zone is indicated by red diagonal zone and white zone and P diffusion zone is indicated by blue diagonal zone.

SIMS surface etching test can determine whether the quaternary interfacial layer is formed between InGaAs and GaAsP layers. The TMGa flow of InGaAs layer and GaAsP layer is 64 and 94 sccm, respectively. SIMS profiles of phosphorus (P), indium (In) and gallium (Ga) for MQWs of three samples and the intensity of element are presented in Fig. 5. Since the element contents are not calibrated corresponding to the standard sample, the tested results are relative values. The periodic variation of elements signal for MQWs confirms that the sputtering rate is constant during the time profiling analysis. The periodic distribution of indium in the three samples indicate the typical MQWs structures. Because the width of indium diffusion or segregation at heterointerface in MQWs is different, as shown in Fig. 5 (labelled both red diagonal zone and white zone), an indium segregation is supposed to occur at the heterointerface during the growth, which may result in 3D growth model instead of 2D, as is proved in Fig. 4(a) by AFM. GaAsP layer is part of white zone and red diagonal zone, which label as indium diffusion width between grey zone (InGaAs layer) and blue zone (GaAsP layer). P diffusion zone is not observed from the heterointerface between GaAsP layer and InGaAs in growth direction except for the first interface of InGaAs/GaAsP, which is attributed to the lower ambient concentration due to the initial sputtering of GaAsP layer, shown as the red diagonal zone in Fig. 5. The diffusion phenomenon observed at the heterointerface can be explained by Fick's law:<sup>33</sup>

$$L^2 = 4Dt \quad (2)$$

where L is diffusion length (nm), and t is time (s). The diffusion coefficient (D) of both the ternary and quaternary materials can be described by the equation (3):

$$D = D_0 \exp(-E_A / kT) \quad (3)$$

where activation energy  $E_A=3.4\pm 0.2$  eV,<sup>33,34</sup> frequency factor  $D_0=3.9$  cm<sup>2</sup>/s,<sup>33</sup> k is the Boltzmann constant and T is growth temperature. Owing to reduced atomic diffusion activation energy, diffusion coefficient increase by the equation (3) and MQWs grew in 3D model which will lead to periodic repeatability get worse and indium diffusion width altered, as shown in Fig. 5(a). It can be seen from the Fig. 5(b, c), the diffusion width of indium increases gradually from right to left, and interface diffusion width is wider in Fig. 5(c) than in Fig. 5(b). The varied diffusion width is resulted from the interaction between accumulation mismatch and thermal diffusion. The increase in diffusion coefficient is mainly caused by two reasons: the increase of accumulation mismatch and the growth temperature.

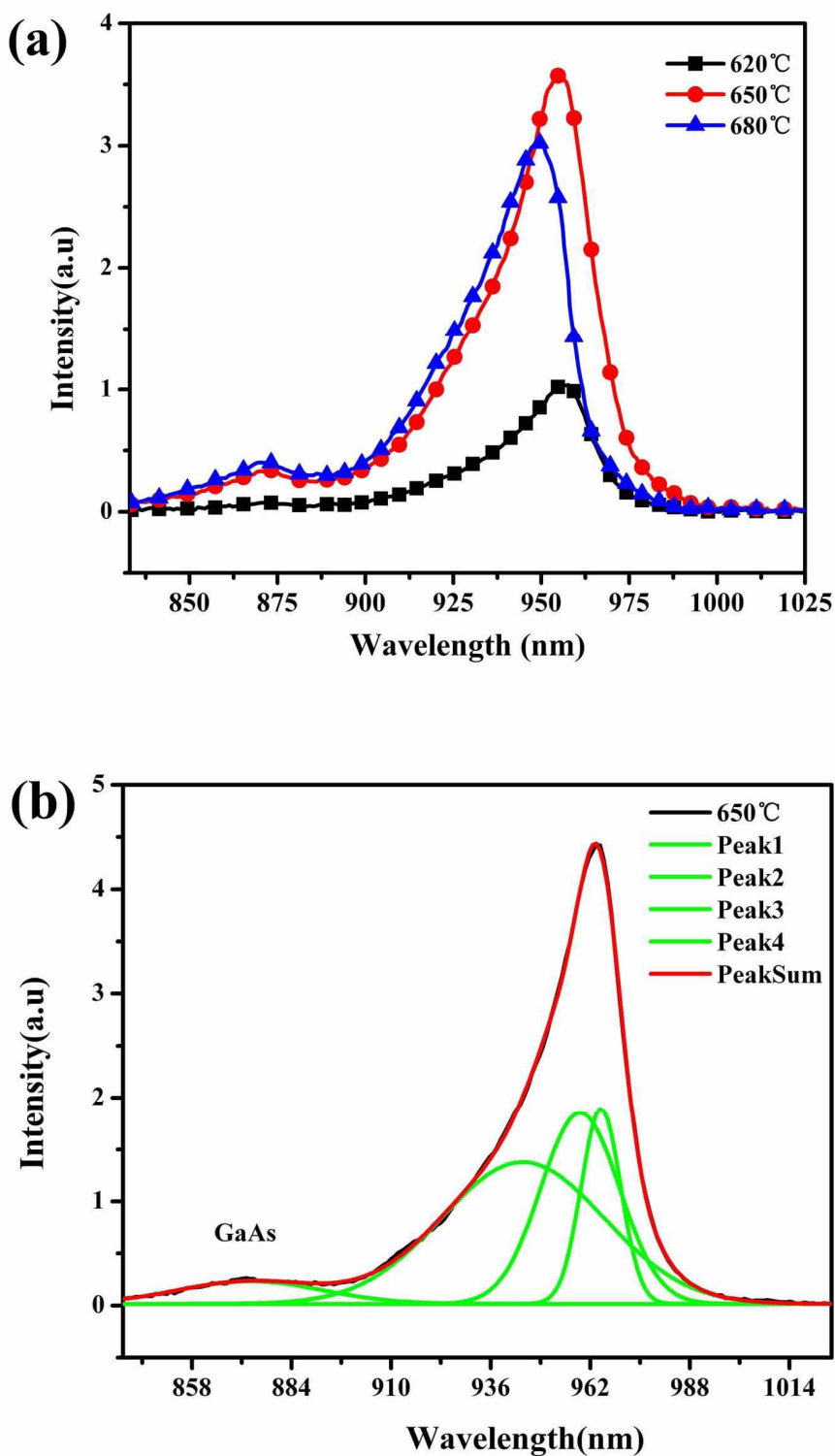


**Fig. 6** PL spectra of InGaAs/GaAsP MQWs depending on different growth temperatures (620 °C, 650 °C and 680 °C), and three samples were excited with a 532 nm laser and the excitation power was 482 mW/cm<sup>2</sup> (a); resolution of overlapped peaks of sample 650 °C using multiple peak fit software (b).



The FWHM of the PL spectrum of quantum well is an important index for assessing heterogeneous interface roughness. From the results of PL spectrum of three samples, the FWHM of PL spectrum of the sample 650 °C is shown to be much narrower as mentioned in Fig. 6(a), which indicates that heterogeneous interface quality is significantly improved at optimized growth temperature under uniform source and heat fluxes. Meanwhile, the overall PL peak could be a combination of several peaks by gaussian peaks. As can be observed in Fig. 6(b), the overall profile of sample 650 °C was resolved using multiple peak fit software. The different spectral positions are resulted from different InGaAs wells thicknesses caused by indium diffusion at the heterointerface, which agrees with the result reported in literature.<sup>35</sup>

The blue shift phenomena of emission peaks are observed by changing growth temperature from 620 °C to 680 °C, as shown in Fig. 5. It could be explained by indium segregation, indium desorption and In-Ga intermixing. A concrete analysis is proposed in the following equations:<sup>36</sup>

$$R = 1 / \exp(E_s / kT) \quad (4)$$

where  $E_s$  is segregation energy.

Desorption rate equation is expressed as:

$$P_{des} = N \exp(-E_{des} / kT) \quad (5)$$

where  $N$  is surface atom concentration,  $E_{des}$  is desorption activation energy.

From equations (4) and (5), segregation coefficient  $R$  increases with growth temperature. It is well known that indium atoms desorbed from InGaAs layer increase with increasing temperature so as to indium composition decrease, which causes blue shift of PL peak. The PL intensity of MQWs is very weak at the low growth temperature (620 °C). Because more impurities are incorporated into MQWs, the crystal quality gets worse at low growth temperature, which seriously affects the luminous intensity of device.<sup>37</sup> Increase the growth temperature to 650 °C, which can enhance the PL intensity and narrow FWHM, resulting in better interface quality and optical properties. However, further increase in growth temperature (680 °C) results in decreased PL intensity and broadened FWHM probably because of the formation of quaternary InGaAsP thin layers by indium diffusion between the upper interface of InGaAs/GaAsP in growth direction, so MQWs interface quality deteriorates and crystal defects are introduced.<sup>38</sup> InGaAsP thin layers decrease confinement ability of barriers so that the probabilities of the photoexcited carrier escape from the quantum well and the nonradiative carrier recombination increased.<sup>39,40</sup>

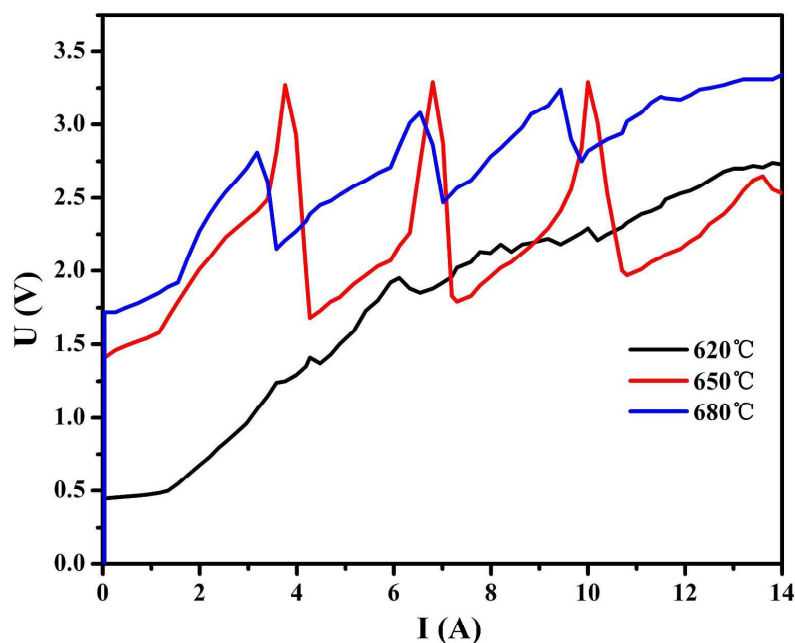


**Fig. 7** Typical I-V curves for InGaAs/GaAsP MQWs were measured at room temperature.

The observed characteristics of current-voltage curves are shown in Fig. 7 for the three samples grown at different temperatures. Negative differential resistance features in MQWs can be observed by adjusting current from 0 to 14 A at room temperature, and the phenomenon was also reported by Shewchuk et al. in GaAs/Al<sub>x</sub>Ga<sub>1-x</sub>As heterostructure.<sup>41</sup> The asymmetry may be due to slightly different barrier thicknesses, and also the interface states at the InGaAs-GaAsP interface. The peak-to-valley ratio from sawtooth-like current-voltage curves manifest negative differential resistance features, which can be expected to be used in semiconductor laser, light emitting diodes, and optoelectronic device.<sup>42</sup> The peak-to-valley maximal ratio is 2.1:1 for the sample 650 °C, as shown in Fig. 6, which indicates better electrical properties of MQWs. For the MQWs grown at low temperature (620 °C), the impurity and carrier concentration increases, the potential barrier becomes higher, the negative resistance effect of MQWs is not obvious, and current-voltage curve varies irregularly. For MQWs grown at high temperature (680 °C), the negative resistance effect becomes weak but current-voltage curve varies regularly, which is attributed to the increased defects and low carrier concentration.<sup>43</sup> From Fig. 7, we observed the threshold voltages of samples at growth temperatures 620 °C, 650 °C and 680 °C are 0.4, 1.3 and 1.7 V, respectively, measured by a fiber optic spectrometer. It indicates the equivalent internal resistance increase as the growth temperature increase. However, the negative differential resistance features are not observed from the I-V curves measured by solar simulator, reported by Sodabanlu et al.<sup>22</sup> That is because the different growth structure and test equipment. But



the varied tendency of the threshold voltages at different growth temperature is consistent with and the open circuit voltages measured by solar simulator.

## Conclusion

In conclusion, we studied the influence of growth temperature on interfacial quality, surface smoothness, and indium diffusion of InGaAs/GaAsP MQWs grown by MOCVD. By adjusting the growth temperature, it is found that the interfacial quality of MQWs grown at 650 °C is optimum. In case of different temperatures, the tradeoff between MQWs abruptness and crystal quality should be carefully considered. The growth of abrupt interface in MQWs indeed requires low temperature in order to decrease indium diffusion length. The existence of indium diffusion zone (InGaAsP) between InGaAs and GaAsP in growth direction reveals the different diffusion width as a result of different growth temperature and accumulated strain. Through current-voltage curves (I-V) measurement of MQWs, the current self-oscillations at room temperature was observed which can be attributed to the negative differential resistance effect, and the higher peak-to-valley voltage ratio of 2.1:1 was obtained at growth temperature 650 °C.

## Acknowledgements

This work was financially supported by the National Natural Science Foundation of China (Grant No.51002102), Shanxi Province Science and Technology Innovation Team Project (Grant No.2012041011).

## References

- 1 N. Y. Jin-Phillipp, F. Phillipp, T. Marschner and W. Stolz, *J. Mater. Sci.: Mater. Electron.*, 1997, **8**, 289.
- 2 H. Fujii, H. Sodabanlu, M. Sugiyama and Y. Nakano, *J. Cryst Growth*, 2015, **414**, 3.
- 3 L. Zhou, X. Gao, L. Y. Xu, Z. L. Qiao and B. X. Bo, *Solid-State Electron.*, 2013, **89**, 81.
- 4 N. K. Dutta, W. S. Hobson, D. Vakhsoori, H. Han, P. N. Freeman, J. F. Jong, J. Lopata, *IEEE Photon. Technol. Lett.*, 1996, **8**, 852.
- 5 M. Bosi and C. Pelosi, *Prog. Photovoltaics: Res. Appl.*, 2007, **15**, 51.
- 6 Y. Wen, Y. P. Wang, M. Sugiyama and Y. Nakano, *Photovoltaic Specialists Conference (PVSC), 2012 35th IEEE*, 2010, 000385.
- 7 Y. Liu and X. R. Xiao, *J. Phys. Chem. B*, 1999, **103**, 10421.

- 8 J. C. Dries, M. R. Gokhale and S. R. Forrest, *Appl. Phys. Lett.*, 1999, **74**, 2581.
- 9 K. Bacher, S. Massie and M. Seaford, *J. Cryst. Growth*, 1997, **175/176**, 977.
- 10 J. P. Samberg, C. Z. Carlin, G. K. Bradshaw, P. C. Colter and S. M. Bedair, *J. Electron. Mater.*, 2013, **42**, 912.
- 11 J. P. Samberg, H. M. Alipour, G. K. Bradshaw, C. Z. Carlin, P. C. Colter, J. M. LeBeau, N. A. El-Masry, S. M. Bedair, *Appl. Phys. Lett.*, 2013, **103**(7), 071605-1.
- 12 Y. P. Wang, R. Onitsuka, M. Deura, W. Yu, M. Sugiyama and Y. Nakano, *J. Cryst. Growth*, 2010, **312**, 1364.
- 13 A. Jasik, A. Wnuk, J. Gaca, M. Wojcik, A. Wojcik-Jedlinska, J. Muszalski and W. Strupinski, *J. Cryst. Growth*, 2009, **311**, 4423.
- 14 T. F. Kuech and R. Potemski, *Appl. Phys. Lett.*, 1985, **47**, 821.
- 15 A. Jasik, A. Wnuk, A. Wójcik-Jedlińska, R. Jakiela, J. Muszalski, W. Strupiński and M. Bugajski, *J. Cryst. Growth*, 2008, **310**, 2785.
- 16 T. Nakano, T. Shioda, E. Abe, M. Sugiyama, N. Enomoto, Y. Nakano and Y. Shimogaki, *Appl. Phys. Lett.*, 2008, **92**, 112106-1.
- 17 K. Muraki, S. Fukatsu, Y. Shiraki and R. Ito, *Appl. Phys. Lett.*, 1992, **61**, 557.
- 18 K. Radhakrishnan, S. F. Yoon, R. Gopalakrishnan and K. L. Tan, *J. Vac. Sci. Technol. A*, 1994, **12**, 1124.
- 19 K. Yamaguchi, T. Okada and F. Hiwatashi, *Appl. Surf. Sci.*, 1997, **117/118**, 700.
- 20 C. Ebert, Z. Pulwin, C. L. Reynolds Jr, D. Shahrjerdi, T. A. Rawdanowicz and D. Dyer Photovoltaic Specialists Conference (PVSC), 2012 38th *IEEE*, 2012, 001465.
- 21 S. J. Ma, Y. P. Wang, H. Sodabanlu, K. Watanabe, M. Sugiyama and Y. Nakano, *J. Cryst. Growth*, 2013, **370**, 157.
- 22 H. Sodabanlu, Y. P. Wang, K. Watanabe, M. Sugiyama and Y. Nakano, *J. Appl. Phys.*, 2014, **115**, 233104-1.
- 23 M. Kitamura, M. Nishioka, R. Schur and Y. Arakawa, *J. Cryst. Growth*, 1997, **170**, 563.
- 24 T. Walther, A. G. Cullis, D. J. Norris and M. Hopkinson, *Phys. Rev. Lett.*, 2001, **86**, 2381.
- 25 Y. H. Kwon, G. H. Gainer, S. Bidnyk, Y. H. Cho, J. J. Song, M. Hansen and S. P. DenBaars, *Appl. Phys. Lett.*, 1999, **75**, 2545.
- 26 J. C. Zhang, D. S. Jiang, Q. G. Sun, G. F. Wang, Y. T. Wang, J. P. Liu, J. L. Chen, R. Q. Jin, J. J. Zhu, H. Yang, T. Dai, Q. J. Jia, *Appl. Phys. Lett.*, 2005, **87**, 071908.

- 27 X. G. He and M. Razeghi, *J. Appl. Phys.*, 1993, **73**(7): 3284.
- 28 Z. Pan, Y. T. Wang, Y. Zhuang, Y. W. Lin, Z. Q. Zhou, L. H. Li, R. H. Wu and Q. M. Wang, *Appl. Phys. Lett.*, 1999, **75**(2), 223.
- 29 S. A. Stepanov and E. A. Kondrashkina, *Phys. Rev. B*, 1998, **57**(8), 3959.
- 30 I. J. Fritz, D. R. Myers, G. A. Vawter, T. M. Brennan and B. E. Hammons, *Appl. Phys. Lett.*, 1991, **58**, 1608.
- 31 Y. Wang, R. Onitsuka, M. Deura, W. Yu, M. Sugiyama and Y. Nakano, *J. Cryst. Growth*, 2010, **312**, 1364.
- 32 J. C. Harmand, M. Juhel, *Appl. Phys. Lett.*, 1993, **62**(25), 3300.
- 33 S. S. Rao, W. P. Gillin and K. P. Hornewood, *Phys. Rev. B*, 1994, **50**(11), 8071.
- 34 A. Oster, F. Bugge, S. Gramlich, M. Procop, U. Zeimer and M. Weyers, *Mater. Sci. Eng. B*, 1997, **44**(1), 20.
- 35 J. F. Zheng, J. D. Walker, M. B. Salmeron and E. R. Weber, *Phys. Rev. Lett.*, 1994, **73**(2), 368.
- 36 A. A. Marmalyuk, O. I. Govorkov, A. V. Petrovsky, D. B. Nikitin, A. A. Padalitsa, P. V. Bulaev, I. V. Budkin and I. D. Zalevsky. *J. Cryst. Growth*, 2002, **237-239**, 264.
- 37 M. M. Karow, N. N. Faleev, A. Maros, C. B. Honsberg, *J. Cryst. Growth*, 2015, **425**, 49.
- 38 J. P. Samberg, H. M. Alipour, G. K. Bradshaw, C. Z. Carlin, P. C. Colter, J. M. LeBeau, N. A. El-Masry and S. M. Bedair, *Appl. Phys. Lett.*, 2013, **103**(7), 071605.
- 39 T. Aihara, A. Fukuyama, H. Suzuki, H. Fujii, M. Sugiyama, Y. Nakano and T. Ikari, *J. Appl. Phys.*, 2015, **117**(8), 084307.
- 40 K. Watanabe, Y. Wang, H. Sodabanlu, H. Sodabanlu, M. Sugiyama and Y. Nakano, *J. Cryst. Growth*, 2014, **401**, 712.
- 41 T. J. Shewchuk, P. C. Chapin and P. D. Coleman, *Appl. Phys. Lett.*, 1985, **46**, 508.
- 42 T. P. E. Broekaert, W. Lee and C. G. Fonstad, *Appl. Phys. Lett.*, 1988, **53**(16), 1545.
- 43 X. R. Wang and Q. Niu, *Phys. Rev. B.*, 1999, **59**(20), R15755.